Experimental studies and mathematical modeling of decolorization of Reactive Orange 16 in packed column

R. Muralikrishnan*, C. Jodhi

*Department of Civil Engineering, Annamalai University, Tamil Nadu – 608002, India, Tel. +91 96552 23113;
emails: murali660105@gmail.com (R. Muralikrishnan), jee.ezhiljodhi@gmail.com (C. Jodhi)*

ABSTRACT

A continuous study was carried out in the up-flow packed bed column to remediate the Reactive Orange 16 (RO16) using biochar derived from coconut shell as a low-cost adsorbent. The sorption mechanism in the continuous process was carried out by studying the influencing parameters namely bed depth, solute flow rate and initial dye concentration. The continuous study explored a maximum uptake capacity of 46.63 mg/g at a bed depth of 25 cm, a flow rate of 0.3 L/h and an initial dye concentration of 100 mg/L. Mathematical modeling such as the Thomas model, modified dose–response model and Yoon–Nelson model was performed to fit the experimental data. Regeneration studies were carried out using 0.01 M NaOH and resulted in 99.7% desorption efficiency. The sorption–elution study concluded that the biochar can undergo three sorption–elution cycles.

Keywords: Biochar; Dyes; Elution; Packed column; Sorption

1. Introduction

In the modern world, the increased usage of water has become one of the most important problems for the environment. Water that was used for domestic and industrial purposes was increasing continuously and results in the generation of a huge quantity of wastewater. Many pollutants such as toxic metals, dye molecules, pesticides, humic substances and many other non-biodegradable substances are mixed in wastewater and thus affect the aquatic ecosystem [1]. Of these different types of pollutants, dyes are considered as one of the important pollutants [2]. Since dyes are used in large quantity in textile industries for different purposes and they can easily interact with the materials, which have been used [3]. Dyes are generally poisonous and cancer-causing agents [4,5]. Release of the dye-bearing wastewater to the surface water streams or rivers will adversely affect the water bodies and makes the water unsuitable for the domestic purpose. These will result in the water demand for domestic purposes and the availability of freshwater was depleted day by day. So,

these wastewaters are to be treated properly before it was discharged from the industries. But the associated treatment cost was a big challenge. Many physical and chemical treatment methods are available but these methods are not cost-effective. But there are certain limitations and difficulties in the existing dye removal methods in the real wastewater system [6]. One of the commonly used treatment methods was adsorption using activated carbon. But the high cost, the problem in the regeneration of the activated carbon was one of the main problems [7,8].

To overcome the disadvantage of the activated carbon, recent research was focused on the production of biochar from the waste materials and it was playing a very important role in the remediation of environmental pollution [9,10]. Biochar is a carbon-rich material produced in the absence of oxygen at varying pyrolysis temperature [11]. Many researches have proved in the past, the biochar can remediate toxic metals [12], dyes [13,14] and other pollutants present in the wastewater in batch mode operation [15]. But the remediation of these pollutants using biochar in a continuous study was very much limited. The objective of the current investigation was to utilize biochar derived from coconut shells for the remediation of Reactive Orange

* Corresponding author.

16 (RO16) in a packed bed column. This study also explored the influence of different operating parameters such as varying bed depth, flow rate and initial dye concentration.

2. Materials and methods

2.1. Biochar synthesis and chemicals

The biochar used in the present study is produced from coconut shells and collected from agricultural lands of Chidambaram, Tamil Nadu, India. The collected coconut shell was rinsed with distilled water to remove the impurities and dried for 24 h under natural drying. The coconut shell was shredded into 7.5 mm size and a measured quantity of 50 g of sample was taken for the synthesis of biochar. This sample was kept in a muffle furnace for 2 h at a heating rate of 5°C/min at the desired temperature of 450°C. The muffle furnace was initially purged with nitrogen gas at a flow rate of 1,000 mL/min to ensure the absence of oxygen inside the muffle furnace. Reactive Orange 16 (RO16) with an empirical formula of $C_{20}H_{17}N_3Na_2O_{11}S_3$; color index of 17,757; the molecular weight of 617.54 g/mg and λ_{max} of 490 nm was used in the current adsorption studies and it was procured from Sigma-Aldrich (India).

2.2. Continuous study

To check the ability of the biochar in the remediation of Reactive Orange 16 (RO16) in the continuous process, a packed bed column was selected. As suggested by Pushpa et al. [16], acrylic glass was used for the continuous setup with a total height of 33 cm with an internal diameter of 1.9 cm. At the bottom of the column, a stainless steel sieve of 0.05 cm is placed followed by glass wool. Also, a circular bead with a diameter of 0.15 cm was placed to a height of 2 cm from the bottom of the column to ensure the steady flow throughout the column. Fig. 1 shows the schematic presentation of the packed bed column.

2.2.1. Impact of biochar bed depth

To study the effect of bed depth on the sorption of 16 Reactive Orange onto the biochar, varying depths

1 - Dye solution
2 - Elutant
3 - Peristaltic pump
4 - Glass wool
5 - Glass beads
6 - Biosorbent
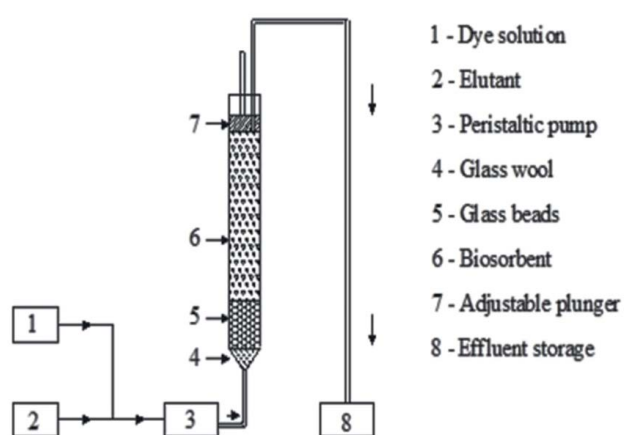7 - Adjustable plunger
8 - Effluent storage

Fig. 1. Packed bed for dye removal using biochar.

of 15, 20 and 25 cm were maintained. Other parameters such as the solute flow rate of 0.3 L/h and the initial concentration of 100 mg/L were maintained.

2.2.2. Impact of solute flow rate

To study the effect of solute flow rate on the sorption of Reactive Orange 16 onto the biochar, the varying flow rate of 0.3, 0.48 and 0.6 L/h were maintained. Other parameters such as biochar bed depth of 25 cm and an initial concentration of 100 mg/L are maintained.

2.2.3. Impact of initial dye concentration

To study the effect of initial dye concentration on the sorption of Reactive Orange onto the biochar, varying initial dye concentrations of 50, 75 and 100 mg/L were maintained. Other parameters such as biochar bed depth of 25 cm and a flow rate of 0.3 L/h are maintained.

2.3. Desorption and regeneration of green seaweed-derived biochar

Once the sorption was completed, desorption studies were carried out to check the possibility of the biochar for consecutive sorption–elution cycles. Desorption studies were carried out using 0.01 M NaOH as the elutant with a flow rate of 0.6 L/h. The samples were collected at the top of the column at regular time intervals and the concentration was measured using a spectrophotometer. The desorption studies were stopped once the exit dye concentration reaches 2% of the inlet concentration (2 mg/L) [16].

2.4. Analysis of column data

To analyze the amount of dye sorbed in the packed bed column by the biochar, parameters such as overall sorption zone (Δt) [17], the volume of effluent treated (V_{eff}) [18], the total quantity of dye molecules pumped (m_{tot}) [18], elution efficiency (E) [16] and a total percentage of dye removed [19] were calculated using Eqs. (1)–(5). A plot of C/C_0 vs. t is used to understand the overall sorption mechanism in the packed column. Other parameters such as the amount of dye remained in the column (m_{adsor}) and column sorption uptake were calculated as suggested by Volesky et al. [18], and Amin et al. [3].

$$\Delta t = t_e - t_b \tag{1}$$

$$V_{eff} = F \cdot t_e \tag{2}$$

$$m_{tot} = \frac{C_0 \cdot F \cdot t_e}{1,000} \tag{3}$$

$$\text{Total dye removal } (\%) = \frac{m_{adsor}}{m_{tot}} \times 100 \tag{4}$$

$$E(\%) = \frac{m_{desor}}{m_{adsor}} \times 100 \tag{5}$$

where t_e is the exhaustion time (min), t_b is breakthrough time (min), the time needed for exit dye concentration to reach 2 mg/L (2% of the inlet dye concentration), F is the flow rate of the solute (mL/min or L/h), C_0 is the inlet concentration (mg/L), C is the outlet concentration m_{desor} is the total dye mass eluted.

2.4.1. Modeling of column data

Several models such as Thomas model, modified dose–response model and Yoon–Nelson model were used to validate the sorption mechanism in a packed bed column and it is given in Eqs. (6)–(8).

Thomas model:

$$\frac{C}{C_0} = 1 + \exp\left(\frac{k_{TH}}{F}\left(Q_0 M - C_0 V_{eff}\right)\right) \tag{6}$$

Modified dose–response model:

$$\frac{C}{C_0} = 1 - \frac{1}{1 + \left(\dfrac{V_{eff}}{b_{mdr}}\right)^{a_{mdr}}} \tag{7}$$

Yoon–Nelson model:

$$\frac{C}{C_0} = \frac{\exp\left(k_{YN}t - \tau k_{YN}\right)}{1 + \exp\left(k_{YN}t - \tau k_{YN}\right)} \tag{8}$$

where Q_0 is the dye sorption capacity (mg/g); k_{TH} is the rate constant of the Thomas model (L/mg h); V_{eff} is the volume of dye solution (L); a_{mdr} and b_{mdr} are the model constants of the modified dose–response model; τ is the Yoon–Nelson constant (min), k_{YN} is the rate constant of the Yoon–Nelson model (1/min).

2.5. Biochar characterization

2.5.1. Analytical methods

To understand the thermal decomposition of the sample, a thermogravimetric analyzer (TG-DSC/NETZSCH STA 449 F3 Jupiter) was used. The analysis was carried out by using a reference sample of alumina (7.668 mg) and a testing sample of coconut shell (8.318 mg) at the desired temperature starting from 0°C to 700°C at a heating rate of 5°C/min and to maintain the inert environment nitrogen gas is purged at a flow rate of 20 mL/min. To understand the surface morphology and chemical composition of the material, scanning electron microscopy equipped with energy dispersive spectroscopy (FEI-Quanta FEG 200F) was used. The samples were coated with a thin layer of gold before measurements. The presence of surface functional groups was analyzed using a Fourier transform infrared (FT-IR) spectrophotometer (Bruker-FTIR/ATR). Potassium bromide (KBr) was added to the dried sample of biochar to form the pellet before measurement.

3. Result and discussion

3.1. Thermogravimetric analysis

The thermogravimetric analyses were conducted to study the impact of pyrolysis on the biomass of the raw coconut shell sample. The degradation curve showed that with an increase in temperature weight loss increased (Fig. 2). A total weight loss of 95.08% occurred at 699°C. The thermal decomposition of the coconut shell was divided into three stages. the first stage occurred between 0°C and 100°C with an overall mass change of 9.38% and this may be due to the moisture loss. The second stage was found to be the massive degradation zones with a mass change of 50.14% that occurred between 100°C and 350°C; this
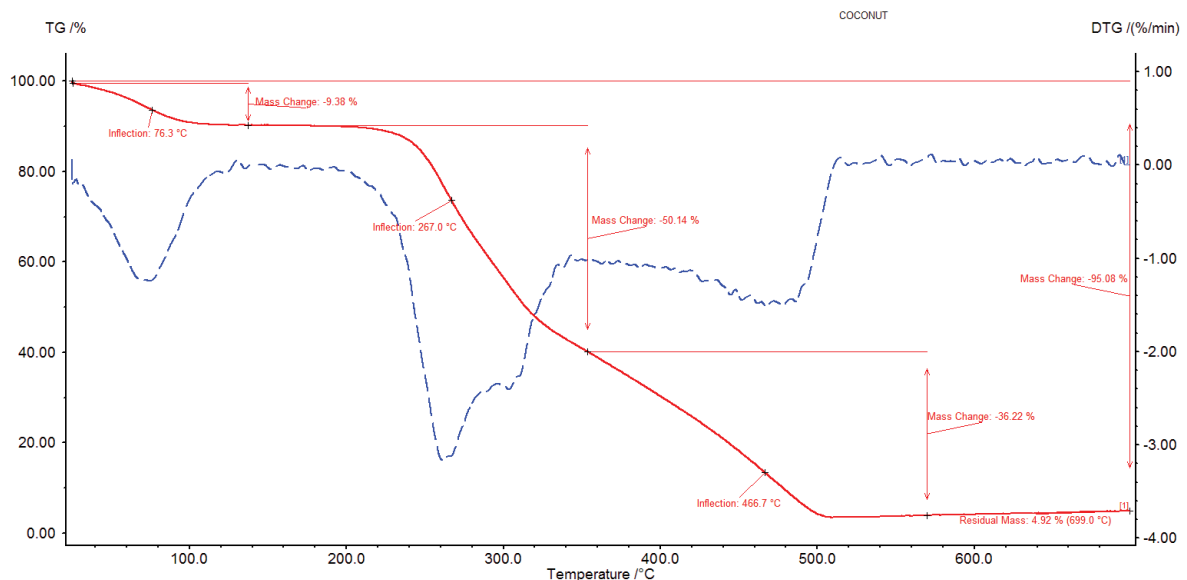

Fig. 2. Thermogravimetric analysis for raw coconut shell.

degradation zone was found to be the most important zone in the pyrolysis process since water-bound, a partial amount of cellulose, hemicellulose and lignin will undergo decomposition [20]. The last stage was the final decomposition zone where almost all the cellulose, hemicellulose and lignin content were decomposed with a mass change of 36.02% between 350°C to 500°C followed by a flat curve with a leftover mass of 4.99% at 699°C.

3.2. Scanning electron microscope with EDS

Fig. 3 shows the surface morphological characteristics of reactive dye and dye bounded biochar using a scanning electron microscope. From Fig. 2, it was clear that the coconut shell derived biochar has a rough surface with a lot of pores present on the surface, which will act as the active binding site and increase the surface area for the maximum uptake of reactive dyes during the adsorption process. After the adsorption of reactive dyes, it was noted that considerable changes have occurred on the surface of the biochar and it may be due to the ion exchange between biochar and reactive dyes. It is also evident that the structural composition of Reactive Orange 16 is composed of OH^- and Na^+ ions and the FT-IR spectra confirmed the presence of different functional groups composed of positive and negative charged ions on the surface of the biochar. This has resulted in the ion exchange between the oppositely charged ions present in the dye and the biochar.

Fig. 4 explores the chemical composition of the biochar before and after the treatment of Reactive Orange 16 (RO16). The raw biochar is found to have the highest carbon content of 87.11% and 12.89% of oxygen with a trace element of sodium, aluminium, silicon, phosphorus, potassium. This confirms the presence of several compounds as impurities in the coconut shell derived biochar. The biochar showed a major modification after adsorption of Reactive Orange 16, the carbon content reduced to 85.27% with an oxygen content of 12.36%. The trace elements present in the raw biochar was disappeared, since the impurities present on the surface of the biochar may be washed by the dye molecules.

3.3. FT-IR spectra

The FTIR spectra of the raw biochar and reactive dye-bounded biochar is given in Fig. 5. From the figure, it is concluded that the biochar has several peaks and indicates the biochar is complex. The FTIR spectra of raw coconut shell derived biochar showed the strong bands at 752 (=C–H bend); 1,191 (C–O stretch); 1,583 (C=C Stretch, N–H bend); 2,328 (O–H stretch); 2,650 (C–H bend). After the adsorption process, the FTIR spectra of biochar showed a functional variation between the reactive dye bound biochar and raw
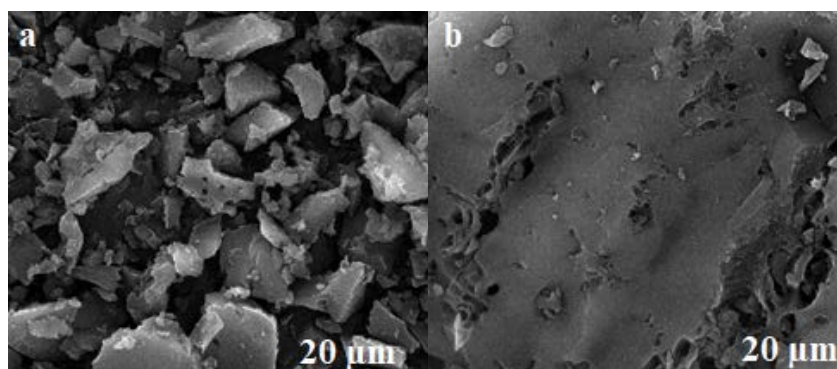

Fig. 3. Scanning electron microscope of coconut shell derived biochar before treatment (a) and after treatment (b).

Element	Wt%	At%
CK	88.11	91.20
OK	10.70	08.32
NaK	00.27	00.15
AlK	00.08	00.04
SiK	00.17	00.08
PK	00.11	00.05
KK	00.53	00.17
CaK	00.02	00.01

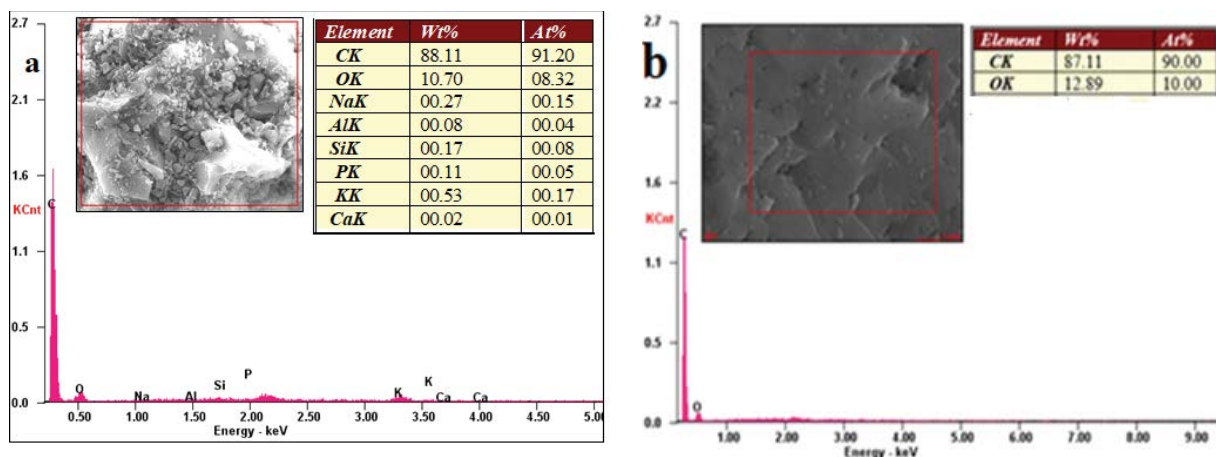| Element	Wt%	At%
CK	87.11	90.00
OK	12.89	10.00

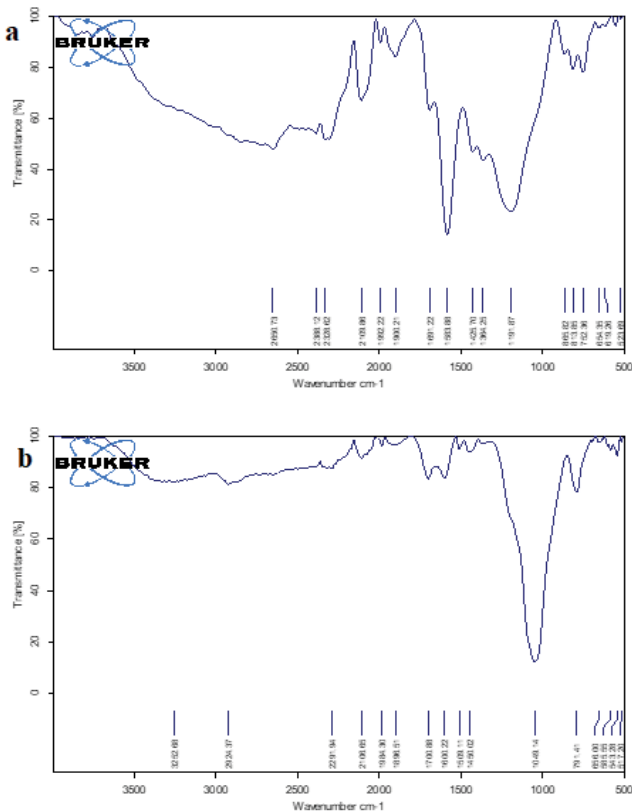Fig. 4. EDS of coconut shell derived biochar before treatment (a) and after treatment (b).

Fig. 5. FT-IR Spectra of coconut shell derived biochar before treatment (a) and after treatment (b).

biochar. For instance, the FTIR spectra of RO16 bound biochar showed a peak at 748 (=C–H bend); 1,182 (C–O stretch); 1,581 C=C stretch; N–H bend); 2,324 (O–H stretch); 2,656 (C–H bend), respectively. Table 2 explores that major shifts occurred during the adsorption of reactive dyes. The presence of sulfonic groups in the reactive dyes, Reactive Orange 16 dye molecules are generally composed of negatively charged ions. The batch results concluded that the initial pH of the sample was measured to be 5.5 and showed less removal efficiency and the maximum removal efficiency was attained at a pH of 2. At acidic conditions, the presence of excess hydrogen ions will bound to the biochar and the biochar may be completely loaded with the positively charged hydrogen ions. This may result in electrostatic attraction between opposite charged ions and favored the adsorption of dye molecules onto the surface of the biochar. On contrary, the biochar derived from coconut shell was mainly composed of many functional groups namely aromatic compounds, alcohols, amides, alkynes and carboxyl groups. These groups will attain positive charge due to ionization under acidic conditions. So, these positively charged ions will attract the negatively charged reactive dye molecules and increase the adsorption capacity of the biochar [21].

3.4. Effect of biochar depth on RO16 sorption

Bed depth plays an important role in the sorption of dyes in a continuous process [16]. So, the experiments were carried out at varying bed depth of 15, 20 and 25 cm at a constant flow rate of 0.3 L/h and an initial concentration of 100 mg/L. To obtain a bed height of 15, 20 and 25 cm in the column, 5.76, 6.42, 6.90 g of coconut shell derived biochar was loaded into the packed bed column. Fig. 6 explored the breakthrough curve obtained for different bed depths with varying time intervals. From Fig. 6, it was also concluded that at higher depth the uptake capacity and removal efficiency was maximum. It was also demonstrating, that increase in bed depth increased the uptake capacity and this was because, at increased bed depth, the available binding site and functional groups present in the biochar favor the maximum sorption of the Reactive Orange 16. For instance, the uptake capacity for 15, 20 and 25 cm was found to be 41.91, 43.85 and 46.62 mg/g with a removal efficiency of 64.89%, 65.36% and 65.29%, respectively. Table 1 shows the column operating parameters at varying bed depths. From the study, it was concluded that the optimum depth for the maximum uptake of Reactive Orange 16 is 25 cm, which is having a treating volume of 4.92 L with an overall sorption zone of 10.9 h.

3.5. Effect of flow rate on RO16 sorption

In real-time industrial wastewater treatment schemes, flow rate plays a very important role in treatment efficiency [22,23]. The effect of flow rate was studied by varying the flow rate as 0.3, 0.48 and 0.6 L/h. Other parameters such as bed depth and initial dye concentration are kept constant as 25 cm and 100 mg/L, respectively. Table 1 summarizes the

Table 1
Column parameters at various bed depth, flow rate and initial RBO3R concentrations during adsorption of RO16

Bed depth (cm)	Flow rate (mL/min)	Initial dye concentration (mg/L)	Uptake (mg/g)	t_b (h)	t_e (h)	Δt (h)	V_{eff} (L)	Total dye removal (%)
15	5	100	41.91	3	12.4	9.4	3.72	64.89
20	5	100	43.85	4.5	14.2	9.7	4.26	65.36
25	5	100	46.62	5.5	16.4	10.9	4.92	65.29
25	8	100	42.54	3.0	9.1	6.1	4.36	67.23
25	10	100	33.99	2	6.25	4.25	3.75	62.45
25	5	75	41.71	6.5	19.8	13.3	5.94	64.51
25	5	50	39.54	9	30.6	21.6	9.18	59.36

Table 2
Parameters predicted by Thomas, modified dose–response and Yoon–Nelson model for adsorption of RO16 in continues studies

| Bed depth (cm)	Flow rate (mL/min)	Initial dye concentration (mg/L)	Thomas model				Modified dose–response model				Yoon–Nelson model			
			Q_0	k_{TH}	R^2	% Error	a_{mdr}	b_{mdr}	R^2	% Error	t	k_{YN}	R^2	% Error
15	5	100	41.45	4.27	0.996	0.51	7.63	3.20	0.990	0.21	8.21	0.78	0.995	0.90
20	5	100	43.66	4.25	0.997	0.42	8.60	3.53	0.996	0.16	9.29	0.80	0.998	0.44
25	5	100	46.55	4.03	0.996	0.41	8.58	3.87	0.999	0.05	10.48	0.73	0.997	0.47
25	8	100	41.89	5.05	0.981	1.54	7.04	3.74	0.992	0.08	6.31	0.97	0.986	0.17
25	10	100	33.70	7.09	0.991	0.67	7.02	3.14	0.993	0.08	4.04	1.49	0.993	0.22
25	5	75	41.63	4.22	0.996	0.41	8.01	4.54	0.999	0.06	12.76	0.55	0.998	0.55
25	5	50	39.43	4.03	0.996	0.41	7.45	6.00	0.999	0.47	17.81	0.37	0.998	1.971
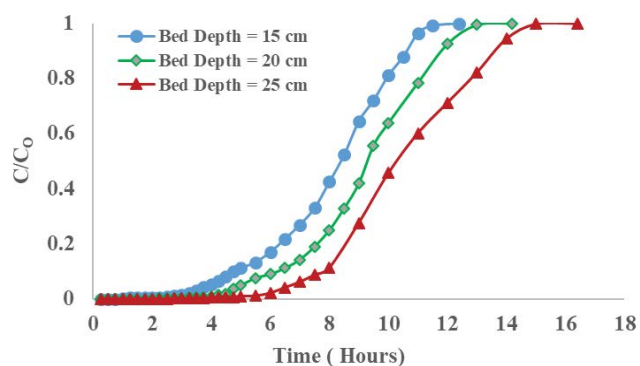
Fig. 6. Effect of bed depth during the sorption of RO16 (process conditions: flow rate = 0.3 L/h and initial concentration = 100 mg/L).
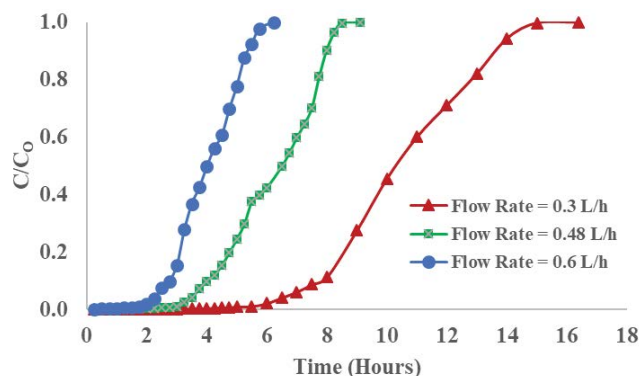

Fig. 7. Effect of flow rate during the sorption of RO16 (process conditions: bed depth = 25 cm and initial concentration = 100 mg/L).

different column parameters obtained for different flow rates. Fig. 7 explores the breakthrough obtained at different flow rates. From Fig. 7, it was clear that at increased flow rate the breakthrough curve obtained very earlier and the resident time was also very less. At a decreased flow rate, the breakthrough curve was following the S-shaped curve and reflects the available time for mass transfer between the dye and the biochar. The uptake capacity of the biochar at different flow rates of 0.3, 0.48 and 0.6 L/h is found to be 46.62, 42.54 and 33.99 mg/g, respectively. It was concluded that the uptake capacity of biochar decreased with an increase in flow rate. At a low flow rate, the biochar and dye will have sufficient time to interact with the binding site and results in maximum uptake and removal efficiency of the dyes [24]. It was also seen that, at low flow rate, the amount of effluent treated was high when compared with the volume of effluent treated at elevated flow rates. So, from the study, it was concluded that the flow rate of 0.3 L/h was considered as the optimum flow rate for the maximum removal efficiency and uptake capacity of biochar.

3.6. Effect of initial concentration on RO16 sorption

Experimental trials were also carried out to study the impact of solute concentration on the biochar in the continuous study. A varying initial concentration of 50, 75 and 100 mg/L at a constant flow rate and biochar depth of

0.3 L/h and 25 cm were maintained. The column operating parameters at different initial concentrations are given in Table 1. Fig. 8 explores the effect of initial dye concentration in the continuous sorption process. At lower dye concentration, due to the presence of excess binding site to the available dye molecules, the breakthrough curve obtained was found to be late and other operating parameters such as exhaustion time, removal efficiency, uptake capacity were also found to be very less when compared with the highest initial concentration [25,26]. The breakthrough curve was found to be sharp when the concentration increased. At the highest concentration of 100 mg/L, the breakthrough was found to be sharp with the highest removal efficiency with less sorption zone. The uptake capacity of the different initial concentrations of 50, 75 and 100 mg/L was found to be 39.54, 41.71 and 46.62 mg/g, respectively.

3.7. Column modeling

To predict the breakthrough curve of wastewater treatment in a packed bed column, a mathematical model is to be compared. In the present study, the Thomas model, Modified dose-response model and Yoon–Nelson model were compared with the experimental data. Of three different models, the Thomas model was one of the popular models in the continuous study since its assumptions are based on Langmuir sorption and elution kinetics [27].
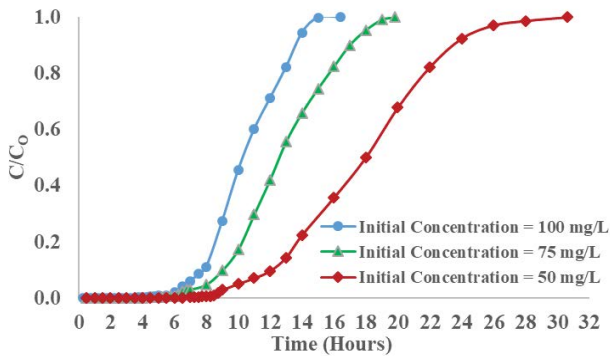
Fig. 8. Effect of initial concentration during the sorption of RO16 (process conditions: bed depth = 25 cm and flow rate = 0.3 L/h).

Fig. 9. Effect of bed depth during the sorption of RO16 (process conditions: flow rate = 0.3 L/h and initial concentration = 100 mg/L).

Figs. 9–11 explored the column breakthrough curve of different models. From Figs. 9–11, it was clear that the modified dose–response model was found to be the best fit model for the experimental data. Table 2 summarises the different constant (Q_0 and k_{TH}) of the model at various operating conditions. From Table 2 it was concluded, the constant value of k_{TH} decreased with an increase in bed depth and initial concentration whereas increased with a decrease in flow rate. The k_{TH} relates the amount of Reactive Orange 16 transferred to the biochar [28,29]. Similarly, the Q_0 values are found to be reversible conditions of k_{TH} values. Q_0 increased with a decrease in bed depth and initial concentration, whereas decreased with an increase in flow rate. These reversible results may be due to the condition, at the highest rate constants biochar adsorption capacity was under-utilized [16]. The Yoon–Nelson model indicates that the decline in the sorption rate for sorbate was equally proportionate to the probability of sorbate adsorption as well as sorbate breakthrough in the column [18]. As shown in Figs. 9–11, the breakthrough curve correlated well with the experimental data.

As suggested by Ramalingam et al. [30], the modified dose–response model was attempted to find the best fit and to overcome the inaccurate data of the Thomas model. Table 2 summarises the parameter constants for the model. The breakthrough curves obtained at different process conditions are given in Figs. 9–11. Based on the correlation coefficient R^2 and error, the modified dose–response model was found to be the best fit model than the other two models. A similar type of result has been observed by Pushpa et al. [16].

3.8. Regeneration studies

Regeneration studies are very important in real-time wastewater treatment since the cost of the treatment is mainly associated with the amount of sorbent used for the adsorption process [31]. So, for a sorbent to be cost-effective, the amount of dye bound to the sorbent is to be regenerated for consecutive sorption cycles [32]. A sorbent mass of 7.05 g with a bed depth of 25 cm, the flow rate of 0.3 L/h is maintained for the sorption–elution cycles. Table 3 summarizes the different column operating parameters for three
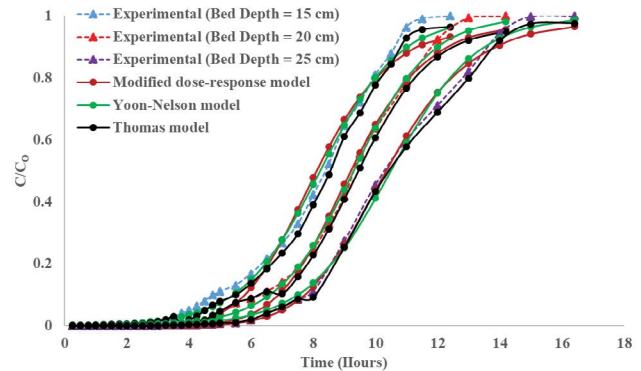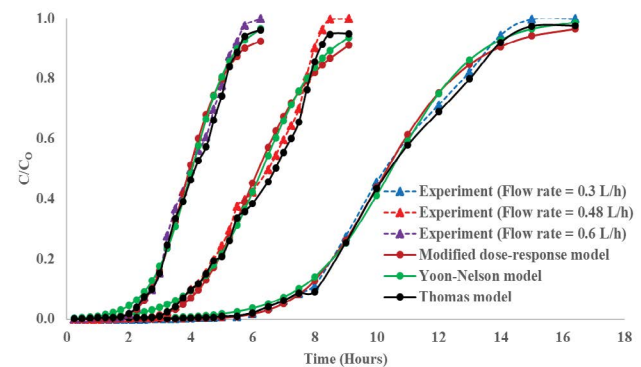

Fig. 10. Effect of flow rate during the sorption of RO16 (process conditions: bed depth = 25 cm and initial concentration = 100 mg/L).
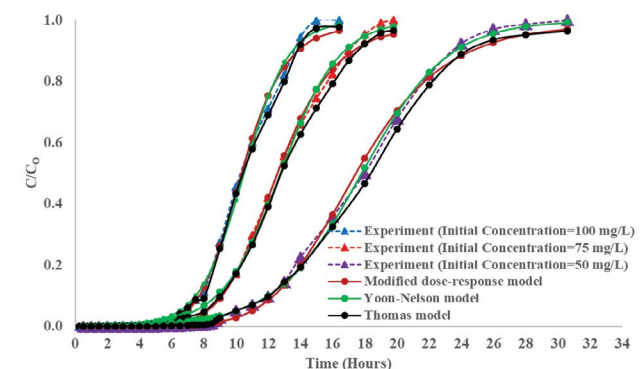

Fig. 11. Effect of initial concentration during the sorption of RO16 (process conditions: bed depth = 25 cm and flow rate = 0.3 L/h).

regeneration cycles. Fig. 12 explores the sorption and elution of RO16 at three consecutive sorption–elution cycles. As the regeneration studies progressed column breakthrough time decreased and exhaustion time increased. This resulted in an increased overall sorption zone, which concludes as the cycle increased the mass transfer zone is increased, which resulted in a decrease in removal

Table 3
Column parameters at three sorption cycles during adsorption of RO16

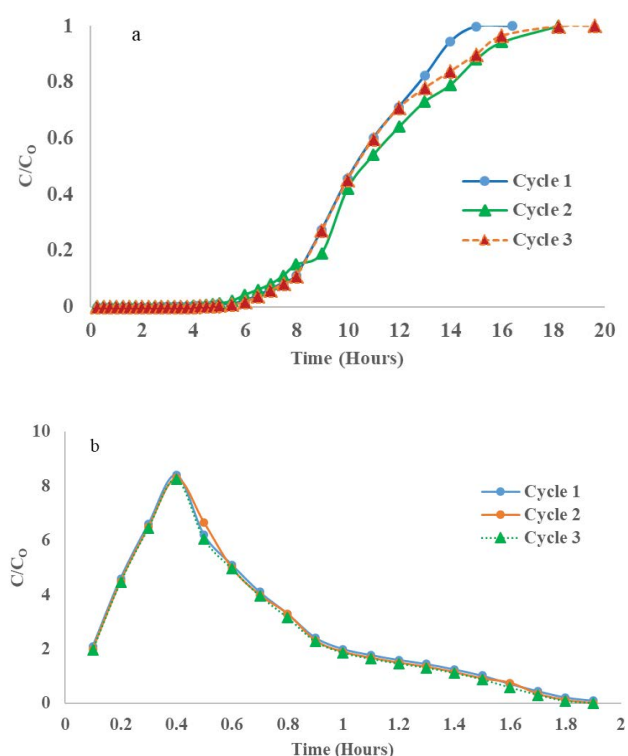| Cycle	Bed depth (cm)	Flow rate (mL/min)	Initial dye concentration (mg/L)	Uptake (mg/g)	t_b (h)	t_e (h)	Δt (h)	V_{eff} (L)	Total dye removal (%)
Cycle 1	15	5	100	46.62	5.5	16.4	10.9	4.92	65.29
Cycle 2	15	5	100	45.59	3.0	18.2	15.2	5.46	60.69
Cycle 3	15	5	100	44.16	2.75	19.6	16.85	5.88	51.74

Fig. 12. Regeneration studies (a) sorption and (b) elution.

efficiency. Table 3 shows that, over the three sorption cycles, the uptake capacity remains almost constant; this concludes that the sorbent can be utilized successfully for three sorption cycles. The results reveal that decrease in adsorption efficiency is not due to the loss of adsorbent but due to the loss of functional groups present in the sorbent [2,33].

Fig. 12 shows the three consecutive elution curves. Elution studies were carried out in an average time of 2 h and the elution process was stopped when the outlet concentration reaches 2 mg/L. Initially, the breakthrough curve raises and suddenly it decreases and the same trend can be seen in all three elution cycles. A high level of RO16 concentration was detected in cycle 1 at a time of 24 min with a C/C_0 value of 8.4. In all three elution cycles, the desorption efficiency was not less than 99.6% and the total volume of 0.01 M NaOH used as elutant is 3.42 L and the total volume of RO16 dye-containing wastewater is found to be 16.26 L and this results in an overall concentration factor of 4.75.

4. Conclusion

From the present study, the following conclusions were summarized.

- A continuous packed bed column was used for the bioremediation of Reactive Orange 16 (RO16). The optimum conditions for the bed depth, flow rate and initial dye concentration were found to be 25 cm, 0.3 L/h and 100 mg/L respectively.
- Maximum uptake of 46.62 mg/g is obtained at optimum conditions.
- Based on the correlation coefficient, modified dose–response model is found to be the best fit model with experimental data and it is always greater than 0.9908.
- The regeneration studies revealed that 0.01 M NaOH can be utilized as a best elutant with three sorption- elution cycles with a desorption efficiency greater than 99.6%.
- So, the coconut shell derived biochar can be successfully utilized as a sorbent for the continuous sorption of Reactive Orange 16 (RO16) in a real wastewater treatment system.

References

[1] R. Gurav, S.K. Bhatia, T.-R. Choi, Y.-K. Choi, H.J. Kim, H.-S. Song, S.M. Lee, S.L. Park, H.S. Lee, J.S. Koh, J.-M. Jeon, J.-J. Yoon, Y.-H. Yang, Application of macroalgal biomass derived biochar and bioelectrochemical system with *Shewanella* for the adsorptive removal and biodegradation of toxic azo dye, Chemosphere, 264 (2020) 128539, doi: 10.1016/j.chemosphere.2020.128539.
[2] G. Ravindiran, R.M. Jeyaraju, J. Josephraj, A. Alagumalai, Comparative desorption studies on remediation of remazol dyes using biochar (sorbent) derived from green marine seaweeds, ChemistrySelect, 4 (2019) 7437–7445.
[3] M. Amin, P. Chetpattananondh, M.N. Khan, Ultrasound assisted adsorption of reactive dye-145 by biochars from marine *Chlorella* sp. extracted solid waste pyrolyzed at various temperatures, J. Environ. Chem. Eng., 8 (2020) 104403, doi: 10.1016/j.jece.2020.104403.
[4] G. Ravindiran, G.P. Ganapathy, J. Josephraj, A. Alagumalai, A critical insight into biomass derived biosorbent for bioremediation of dyes, ChemistrySelect, 4 (2019) 9762–9775.
[5] P. Saravanan, B.P. Thillainayagam, G. Ravindiran, J. Josephraj, Evaluation of the adsorption capacity of *Cocos Nucifera* shell derived biochar for basic dyes sequestration from aqueous solution, Energy Sources Part A, (2020) 1–17, https://doi.org/10.1080/15567036.2020.1800142.
[6] S. Praveen, J. Jegan, T. Bhagavathi Pushpa, R. Gokulan, Sorption kinetics and isotherm studies of cationic dyes using groundnut (*Arachis hypogaea*) shell derived biochar a low-cost adsorbent, Appl. Ecol. Environ. Res., 18 (2020) 1925–1939.
[7] G. Kalyani, S.P. Mahendran, R. Gokulan, Removal of lead metal ion using biowaste of *Pithophora cleveana* wittrock

and *Mimusops elengi*, Energy Sources Part A, (2020), doi: 10.1080/15567036.2020.1831657.

[8] R. Gokulan, G. Ganesh Prabhu, J. Jegan, Remediation of complex remazol effluent using biochar derived from green seaweed biomass, Int. J. Phytorem., 21 (2019) 1179–1189.

[9] R. Gokulan, A. Avinash, G.G. Prabhu, J. Jegan, Remediation of remazol dyes by biochar derived from *Caulerpa scalpelliformis*—an eco-friendly approach, J. Environ. Chem. Eng., 7 (2019) 103297, https://doi.org/10.1016/j.jece.2019.103297.

[10] R. Gokulan, G. Ganesh Prabhu, A. Avinash, J. Jegan, Experimental and chemometric analysis of bioremediation of remazol dyes using biochar derived from green seaweeds, Desal. Water Treat., 184 (2020) 340–353.

[11] J. Jegan, S. Praveen, T.B. Pushpa, R. Gokulan, Biodecolorization of basic violet 03 using biochar derived from agricultural wastes: isotherm and kinetics, J. Biobased Mater. Bioenergy, 14 (2020) 316–326.

[12] E. Singh, A. Kumar, R. Mishra, S.M. You, L. Singh, S. Kumar, R. Kumar, Pyrolysis of waste biomass and plastics for production of biochar and its use for removal of heavy metals from aqueous solution, Bioresour. Technol., 320 (2020) 124278, doi: 10.1016/j.biortech.2020.124278.

[13] A.K. Priya, R. Gokulan, A. Vijayakumar, S. Praveen, Biodecolorization of remazol dyes using biochar derived from *Ulva reticulata*: isotherm, kinetics, desorption, and thermodynamic studies, Desal. Water Treat., 200 (2020) 286–295.

[14] M.E. Mahmoud, A.M. Abdelfattah, R.M. Tharwat, G.M. Nabil, Adsorption of negatively charged food tartrazine and sunset yellow dyes onto positively charged triethylenetetramine biochar: optimization, kinetics and thermodynamic study, J. Mol. Liq., 318 (2020) 114297, doi: 10.1016/j.molliq.2020.114297.

[15] Z. Mahdi, A. El Hanandeh, Q.M. Yu, Influence of pyrolysis conditions on surface characteristics and methylene blue adsorption of biochar derived from date seed biomass, Waste Biomass Valorization, *8 (2017)* 2061–2073.

[16] T.B. Pushpa, J. Josephraj, P. Saravanan, G. Ravindran, Bio-decolorization of basic blue 41 using EM based composts: isotherm and kinetics, ChemistrySelect, 4 (2019) 10006–10012.

[17] R. Gokulan, G. Ganesh Prabhu, J. Jegan, A novel sorbent *Ulva lactuca*-derived biochar for remediation of remazol brilliant orange 3R in packed column, Water Environ. Res., 91 (2019) 642–649.

[18] B. Volesky, J.Weber, J.M. Park, Continuous-flow metal biosorption in a regenerable *Sargassum* column, Water Res., 37 (2003) 297–306.

[19] Z. Aksu, F. Gönen, Biosorption of phenol by immobilized activated sludge in a continuous packed bed: prediction of breakthrough curves, Process Biochem., 39 (2004) 599–613.

[20] T.V.N. Padmesh, K. Vijayaraghavan, G. Sekaran, M. Velan, Application of two- and three-parameter isotherm models: biosorption of acid red 88 onto *Azolla microphylla*, Biorem. J., 10 (2006) 37–44.

[21] L.J. Xia, C. Li, S.J. Zhou, Z. Fu, Y. Wang, P. Lyu, J.J. Zhang, X Liu, C.H. Zhang, W.L. Xu, Utilization of waste leather powders for highly effective removal of dyes from water, Polymers, 11 (2019) 1786, https://doi.org/10.3390/polym11111786.

[22] X.J. Hu, X.B. Zhang, H.H. Ngo, W.S. Guo, H.T. Wen, C.C. Li, Y.C. Zhang, C.J. Ma, Comparison study on the ammonium adsorption of the biochars derived from different kinds of fruit peel, Sci. Total Environ., 707 (2018) 135544, https://doi.org/10.1016/j.scitotenv.2019.135544.

[23] T.V.N. Padmesh, K. Vijayaraghavan, G. Sekaran, M. Velan, Batch and column studies on biosorption of acid dyes on fresh water macro alga *Azolla filiculoides*, J. Hazard. Mater., 125 (2005) 121–129.

[24] Q.-Q. Zhong, X. Xu, L. Shen, Y.-J. Han, Y.-C. Hao, Breakthrough curve analysis of *Enteromorpha prolifera* packed fixed-bed column for the biosorption, Environ. Eng. Sci., 35 (2018) 864–874.

[25] K. Vijayaraghavan, Y.-S. Yun, Competition of Reactive red 4, Reactive Orange 16 and Basic blue 3 during biosorption of Reactive blue 4 by polysulfone-immobilized *Corynebacterium glutamicum*, J. Hazard. Mater., 153 (2008) 478–486.

[26] H.R. Ong, M.R. Khan, A. Yousuf, N. Jeyaratnam, D.M. Reddy Prasad, Effect of waste rubber powder as filler for plywood application, Pol. J. Chem. Technol., 17 (2015) 41–47.

[27] K. Vijayaraghavan, M. Thilakavathi, K. Palanivelu, M. Velan, Continuous sorption of copper and cobalt by crab shell particles in a packed column, Environ. Technol., 26 (2005) 267–276.

[28] H.C. Thomas, Heterogeneous ion exchange in a flowing system,J. Am. Chem. Soc., 66 (1994) 1664–1666.

[29] R. Radhika, T. Jayalatha, G. Rekha Krishnan, S. Jacob, R. Rajeev, B.K. George, Adsorption performance of packed bed column for the removal of perchlorate using modified activated carbon, Process Saf. Environ., 117 (2018) 350–362.

[30] S. Ramalingam, L. Parthiban, P. Rangasamy, Biosorption modeling with multilayer perceptron for removal of lead and zinc ions using crab shell particles, Arabian J. Sci. Eng., 39 (2014) 8465–8475.

[31] G.Y. Yan, T. Viraraghavan, Heavy metal removal in a bio-sorption column by immobilized *M. rouxii* biomass, Bioresour. Technol., 78 (2001) 243–249.

[32] K. Vijayaraghavan, K. Palanivelu, M. Velan, Crab shell-based biosorption technology for the treatment of nickel-bearing electroplating industrial effluents, J. Hazard. Mater., 119 (2005) 251–254.

[33] K. Saravanakumar, R. Senthilkumar, D.M.R. Prasad, B.S. Naveen Prasad, S. Manickam, V. Gajendiran, Batch and column arsenate sorption using *Turbinaria ornata* seaweed derived biochar: experimental studies and mathematical modeling, ChemistrySelect, 5 (2020) 3661–3668.